

UTILIZATION OF STRONG-MOTION DATA FOR ASSESSMENT OF STRUCTURAL INTEGRITY IN INSTRUMENTED HIGHWAY BRIDGES

Virginia Mosquera, Andrew W. Smyth and Raimondo Betti

Department of Civil Engineering and Engineering Mechanics
Columbia University, New York

Abstract

This study focuses on the use of strong motion data recorded during earthquakes and aftershocks to provide a preliminary assessment of the structural integrity and possible damage in bridges. A system identification technique is used to determine dynamical characteristics and high-fidelity first-order linear models of four bridges from low level earthquake excitations. A finite element model (FEM) was developed and updated to simulate data from a damaging earthquake for one of the bridges. The difference between data recorded or simulated by FEM and data predicted by the linear model was used to detect damage. The use of this technique can provide an almost immediate, yet reliable, assessment of the structural health after a seismic event.

Introduction

It is of great interest after an extreme event such as an earthquake, to have reliable information regarding the integrity of a structure. In recent years, the use of vibration based damage detection techniques for structural health monitoring has gained significant attention by researchers. There is a considerable amount of studies on these techniques, where damage is usually determined by a change in the dynamical properties of the structure. Doebling et al. [1] presents a thorough review of these techniques.

An alternative for damage detection is to identify damage by determining the degree of nonlinearity present in the structural response [2]. If a linear model has been previously identified for a healthy state of the structure, this model should be able to accurately predict the response to any other input data if the structure stays in the elastic range. The difference between the recorded data and the response predicted by the linear model can be used to give an estimate of the state of the structure.

There has been a large amount of algorithms developed in the frequency and time domain to identify modal parameters and determine state space representations of linear dynamical systems. Many studies have successfully applied these techniques in the system identification of buildings and bridges [3],[4],[5]. Among those techniques, one that has shown great promise is the Eigensystem Realization Algorithm (ERA) proposed by Juang and Pappa [6], with Observer Kalman Filter Identification [7],[8].

In this study the ERA/OKID is used to identify the modal parameters and linear models of four bridges. The input and output data used for the identification are obtained from previous ground motions and structural responses recorded by the California Strong Motion

Instrumentation Program (CSMIP). One of the bridges was selected for further study and a FEM model was developed for it.

Due to assumptions made while developing a FEM and uncertainty in boundary conditions, geometrical and material properties of the structure, there can be significant differences between the dynamic behavior of the model and the real structure. To accurately represent the structure, the FEM model must be updated [9].

In model updating techniques an objective function is optimized to find a model that behaves similarly to the real structure [10], [11]. Here some structural parameters were varied to match the measured structural responses of the bridge, as well as the modal frequencies found using ERA/OKID. To select the optimum values for these parameters a Genetic Algorithm (GA) optimization approach [12] was used.

After the updating process, hinges which defined the nonlinear behavior of the structure were inserted in the model at the tower-deck and tower-foundation connections as well as in the bent cap on each side of the column. Once the FEM was completed, appropriately scaled input time histories of the ground motion from a previously recorded data set were used to simulate the possible nonlinear response of the bridge to a future damaging earthquake. The simulated time histories of the response from the nonlinear model will represent a new set of data that can be compared with the data predicted by the linear model identified with ERA/OKID and provide an estimate of the location and amount of structural damage that occurs during a major earthquake.

System Identification

State space representation

The dynamic behavior of a multi (n) degree-of-freedom (n DOF) linear structural system can be represented by a system of second order differential equations as:

$$M\ddot{q}(t) + C\dot{q}(t) + Kq(t) = B_2u(t) \quad (1)$$

where $q(t)$ is the structural displacement vector, M , C and K are respectively the $n \times n$ mass, damping and stiffness matrices; $u(t)$ is the input vector and B_2 is the input matrix. When the input is a seismic excitation, the external forcing term $B_2u(t)$ can be replaced by $-M\ddot{q}_g(t)$, where $\ddot{q}_g(t)$ is the ground acceleration.

By defining $2n \times 1$ state vector $x(t)$ as a vector containing the displacement $q(t)$ and the velocity $\dot{q}(t)$, the system of second order differential equations (1) can be rewritten as a first order system of differential equations

$$\dot{x}(t) = A_c x(t) + B_c u(t) \quad (2)$$

$$y(t) = C_c x(t) + D_c u(t) \quad (3)$$

where the matrices A_c , B_c , C_c and D_c are the time invariant continuous time system matrices while $u(t)$, of dimension $r \times 1$, and $y(t)$, of dimension $m \times 1$, are the input and output vectors, respectively. Since the input and output generated by an earthquake excitation will be recorded at discrete time intervals, equations (2) and (3) must also be expressed in discrete time

$$x(k + 1) = Ax(k) + Bu(k) \quad (4)$$

$$y(k) = Cx(k) + Du(k) \quad (5)$$

where $x(k)$, $y(k)$, and $u(k)$ represent the state, output and input vectors, respectively, at time $t = k \Delta t$, with Δt being the sampling time. The matrices A , B , C and D are the discrete time versions of the continuous time matrices A_c , B_c , C_c and D_c .

Eigensystem Realization Theory

A realization is a set of matrices A , B , C and D that describe the behavior of the structure and satisfy equations (4) and (5). A system can have an infinite number of realizations that will predict the same output for a given input: a minimum realization will have the smallest state-space dimensions among all the possible realizations and the modal parameters found will be the ones of the structure.

The ERA algorithm is used to find the minimum realization. This algorithm uses the Hankel matrix, which can be written as:

$$H(k-1) = \begin{bmatrix} Y_k & Y_{k+1} & Y_{k+2} & \dots & Y_{k+\beta+1} \\ Y_{k+1} & Y_{k+2} & Y_{k+3} & \dots & Y_{k+\beta} \\ Y_{k+2} & Y_{k+3} & Y_{k+4} & \dots & Y_{k+\beta-1} \\ \vdots & \vdots & \vdots & \ddots & \vdots \\ Y_{k+\alpha-1} & Y_{k+\alpha} & Y_{k+\alpha} & \dots & Y_{k+\alpha+\beta-1} \end{bmatrix} \quad (6)$$

where Y_k are the Markov parameters, defined as:

$$Y_0 = D \quad (7)$$

$$Y_k = CA^{k-1}B \quad \text{for } k=1,2,\dots \quad (8)$$

while α and β are sufficiently large numbers that determine the size of the Hankel matrix.

For lightly damped systems, the number of Markov parameters can be quite large so to make the computational effort quite cumbersome. To circumvent this problem, the Observer Kalman Filter Identification algorithm transforms the state equations (4) and (5) into observer equations where the observer gain matrix is chosen to make the observer asymptotically stable. In this case, it is much easier to retrieve the observer's Markov parameters and, through a recursive relation, to obtain the system's Markov parameters. Details of this methodology can be found in [4], [7] and [8].

Useful information about the system's dynamics can be obtained by the Singular Value Decomposition (SVD) of $H(0)$, that can be expressed as:

$$H(0) = U\Sigma V^T = \begin{bmatrix} U_n & U_{n_1-n} \end{bmatrix} \begin{bmatrix} S_n & 0 \\ 0 & 0 \end{bmatrix} \begin{bmatrix} V_n \\ V_{n_2-n} \end{bmatrix} = U_n S_n V_n \quad (9)$$

where the matrices U , of dimensions $n_1 \times n_1$, and V , of dimension $n_2 \times n_2$, are orthonormal while Σ is a rectangular matrix, of dimension $n_1 \times n_2$, that contains the singular values of $H(0)$.

By looking at the non-zero singular values contained in the matrix S_n , it is possible to identify the number of vibrational modes that significantly contribute to the dynamic response. If the signals contain very small noise level, the distinction between non zero singular values (corresponding to structural modes) and “almost zero” singular values (noise related modes) is quite evident, allowing a clear estimation of the order of the system. However, if the recorded data have a substantial amount of measurement noise, then the distinction between structural and noise modes is not clear and this requires additional manipulation (e.g. stabilization diagram and/or optimization).

Using the definition of the Markov parameters, the Hankel matrix $H(1)$ and the singular value decomposition of $H(0)$, the state matrix A , the input matrix B and the output matrix C in equations (4) and (5) can be expressed as:

$$A = S_n^{-\frac{1}{2}} U_n^T H(1) V_n S_n^{-\frac{1}{2}} \quad (10)$$

$$B = S_n^{-\frac{1}{2}} V_n E_r \quad (11)$$

$$C = E_m^T U_n S_n^{\frac{1}{2}} \quad (12)$$

where $E_m^T = [I_m \ 0_m \ \dots \ 0_m]$, $E_r = [I_r \ 0_r \ \dots \ 0_r]$, with I_i and 0_i being an identity matrix and a null matrix, respectively, of order i .

Model Updating

Another approach to create a dynamic model of a structural system is to directly determine the mass, damping and stiffness matrices, as they appear in equation (1). This can be accomplished by using the FEM. However, no matter how accurate the initial FEM model, there are always inaccuracies between the dynamic behavior of such a model and the real structure, inaccuracies that can be reduced through model updating. The purpose of model updating is to adjust the parameters of the FEM (e.g. Young's modulus, ultimate strength, boundary conditions, etc.) in a way such that it behaves as close to the real structure as possible. Usually, updating techniques vary the structural parameters of the model so as to minimize an objective function that compares measured and numerical responses (e.g. measured and computed natural frequencies, recorded and predicted time histories of the structural response, etc.). Different techniques have been proposed for this purpose; in this project, a form of Genetic algorithms has been used.

Generic Algorithm

Genetic algorithms have been broadly used as a tool to find an exact or approximate solution for search or optimization problems. Essentially, it is a programming technique that mimics the biological process of natural evolution and survival of the fittest to solve an optimization problem [13].

The Genetic Algorithm was first introduced by John Holland [14], who proposed that each potential solution to a problem can be seen as a set of genes. Usually, a gene is represented by binary bits and the possible solution by a binary string is called chromosome. The evolution process starts from a randomly-generated population of chromosomes. At each cycle, a new set

of chromosomes is generated by recombination and mutation of a previous generation. The purpose of this evolutionary algorithm is to eventually find the fittest chromosome that will lead to the best solution for the problem at hand. All genetic algorithms follow these basic steps:

A set of parameters from the problem are selected to be encoded into a binary string. Once the parameters have been selected, an initial population of chromosomes is randomly generated. A fitness function is selected and evaluated for each member of the population to determine the quality of each solution.

The selection of a chromosome for reproduction is based on its fitness; there are different schemes to select the parent chromosomes, like the roulette-wheel selection and tournament selection among others. In the roulette wheel, the probability to be selected is proportional to the fitness of each chromosome while, in the tournament selection, subgroups of chromosomes are selected and members of each subgroup compete against each other. The latter selection contributes toward the preservation of diversity on the population and it is used here.

Once the parent chromosomes have been selected, the reproduction process is simulated by applying a crossover operator and a mutation operator. The crossover operator tries to simulate the recombination that occurs to chromosomes during reproduction. A position in the binary string is randomly selected and mutually exchanges parts of the string before and after this point to create two offsprings or child chromosomes. The mutation operator is applied in order to improve the fitness and avoid loss of diversity in the population. It involves a random alteration of the genes and it has a small probability of occurrence.

The evolutionary process is repeated until a termination criterion is satisfied. The following termination criteria are commonly used: 1) a maximum number of generations is completed [15],[16], 2) a global minimum within an specified tolerance was found [17], or 3) a maximum number of consecutive generations without improvement was reached [18]. In the problem studied here, the applied termination criterion was the maximum number of generations. The steps described above are illustrated in Fig. 1.

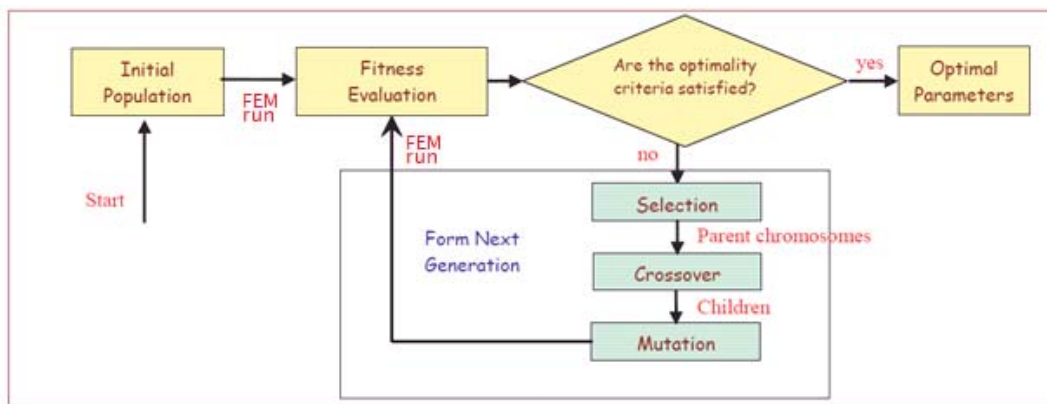


Fig. 1. Genetic Algorithm flowchart

These techniques can also be combined with others such as elitism, which guarantees survival of the fittest chromosome into the next generation; and niching, which allows the possibility of exploring different local optima by creating and evolving smaller subgroups within the population. Another recent technique is the micro-GA [19], [20], which prevents loss of

diversity by restarting the population as soon as it degenerates below some threshold. There is also the sawtooth-GA technique proposed by Koumoussis, and Katsaras [21], which proved to be most helpful for the particular problem considered here. This method uses a variable population size of mean value \bar{n} , and amplitude D , and a periodic partial re-initialization of the population of a period T , in the form of a saw-tooth function as shown in Fig. 2.

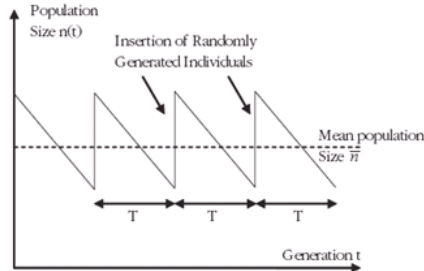


Fig. 2. Population variation scheme of saw-tooth GA.

Analysis of results

When a structure is subjected to a severe seismic event, it will deform into the inelastic range, exhibiting a nonlinear hysteretic behavior. Since the amount of damage experienced by the structure will increase as the inelastic behavior increases, damage can be determined by estimating the degree of nonlinearity present in the response of the bridge.

The linear state-space model identified by ERA/OKID is able to accurately predict the response of the structure at different sensor locations to any ground motion that produces a linear-elastic behavior on the bridge. However, if nonlinear behavior occurs, the model will no longer be able to predict the structural response. The difference between the predicted response and the measured response will be used to determine whether the structure has suffered damage or not. This difference will be quantified by the Root Mean Square (RMS) error

$$\text{RMSerror} = \sqrt{\frac{\sum_1^n (\text{Acc}_{\text{measured}} - \text{Acc}_{\text{predicted}})^2}{\sum_1^n (\text{Acc}_{\text{measured}})^2}} \quad (13)$$

where n is the number of time steps in each acceleration time history.

Experimental results

In this paper four bridges instrumented by CSMIP are studied. . The bridges studied here are a) Rio Dell – Hwy 101/Painter Street Overpass, b) Sylmar – I5/14 Interchange Bridge, c) San Bernardino – I10/215 Interchange and d) El Centro – Hwy 8/Meloland Road Overpass. Initially the modal parameters of each bridge were identified using ERA/OKID. After this identification, the Meloland Road Overpass was selected for further study.

System identification

The Rio Dell overpass is a two span bridge with a length of 265 feet. It is a monolithic, cast in place, prestressed concrete, box girder bridge with end diaphragm abutments and a two column bent. Both end diaphragm abutments and two-column bent are skewed at 39 degrees and supported on piles. It was instrumented in 1977 with 17 strong motion accelerometers along one side of the deck and at the base of one of the piers and 3 accelerometers at the free field. In the

identification process 7 accelerometers along the deck were used as output data and 6 accelerometers at the embankments as input data (Fig. 3a).

The Sylmar interchange bridge is a curved concrete box girder with a length of 1582 feet and a deck width of 51 feet. It has 9 spans supported in single column bents and one expansion joint. The columns are orthogonal, supported by circular CIDH concrete piles. It was constructed and instrumented in 1995. Thirty nine strong motion accelerometers were installed along the deck, abutments and base of the columns, and 3 more at the free field site. For the modal parameter identification 9 channels were used as inputs and 21 channels as outputs (Fig. 3b).

The San Bernardino connector is a curved multi-span concrete box girder with a length of 2540 ft. It has five separation joints that divide the bridge into six segments of different lengths. The superstructure is supported by single column concrete bents; the columns are octagonal in shape and have variable height. The Bridge was constructed in 1973 and it was retrofitted in 1991. In the retrofitting, steel jackets were added to the columns, the foundation were enlarged and cables tying adjacent slabs at the expansion joints were replaced. In 1992 the bridge was instrumented with 37 strong motion accelerometers located along the deck, at the base of the columns and at the free field. Here 12 sensors located at the abutments and base of the columns were used as input data and 22 sensors along the deck of the bridge were used as output data for the modal parameter identification (Fig. 3c).

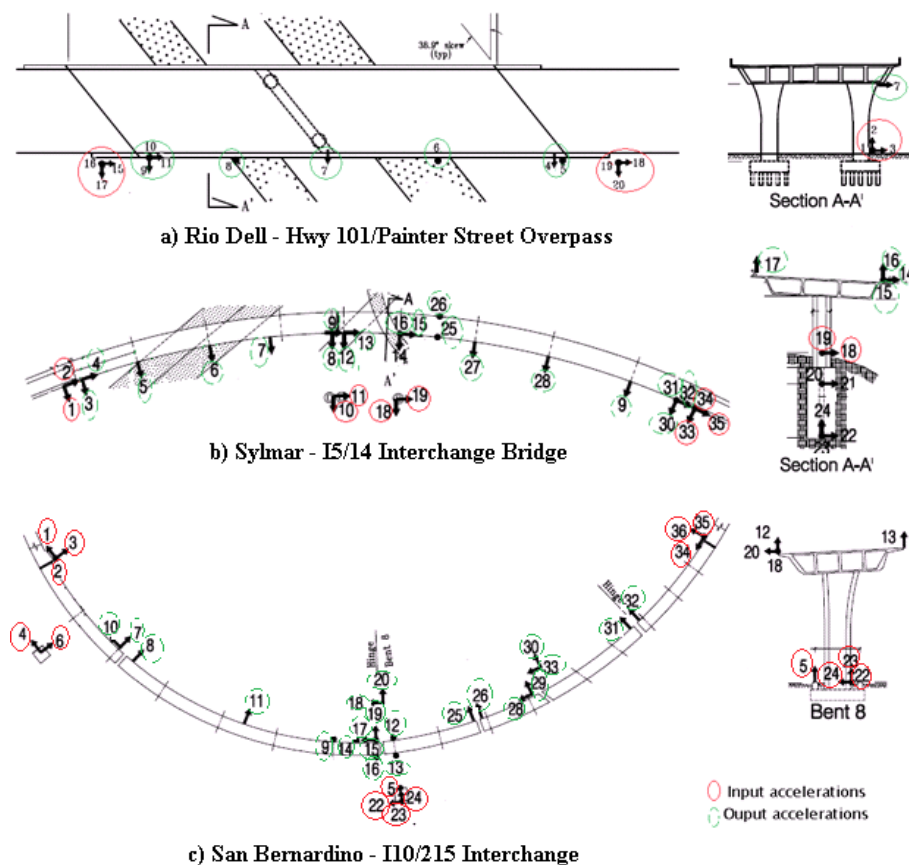


Fig. 3. Plan views and sensor locations of bridges

In the modal parameter identification of the first 3 bridges, two ground motions were used for each bridge and are listed in Table 1. The modal frequencies and damping identified for Rio Dell Overpass, Sylmar Interchange and San Bernardino Interchange are listed in Tables 2, 3 and 4 respectively. Similar frequencies were obtained for each bridge for both sets of ground motions: however, larger differences appear in the identified damping ratios. This is expected since the identification of the damping factors is much more difficult than the identification of the frequency and it is strongly dependent on the order of the identification model.

Table 1. Earthquakes used for system identification.

Bridge	Earthquake	Horizontal Apk(g)	
		Ground	Struct.
Rio Dell	Trinidad	0.147	0.330
	Rio Dell	N/A	0.593
Sylmar	April 11/1999	0.011	0.096
	Jan 14/2001	0.084	0.064
San Bernardino	Yucaipa	0.135	0.244
	Chino hills	0.110	0.165

Table 2. Dynamic parameters identified for Rio Dell Overpass

Mode	Trinidad EQ		Rio Dell EQ	
	ω (Hz)	ξ (%)	ω (Hz)	ξ (%)
1	3.39	2.67	3.36	2.20
2	4.33	9.53	4.14	20.29
3	4.85	2.82	4.91	6.42
4	-	-	5.09	4.21
5	6.08	1.94	-	-
6	7.30	3.17	7.19	10.12

Table 3. Dynamic parameters identified for Sylmar Interchange.

Mode	April 11 / 1999		Jan 14 / 2001	
	ω (Hz)	ξ (%)	ω (Hz)	ξ (%)
1	-	-	0.75	1.94
2	1.04	1.85	1.01	1.14
3	1.31	0.43	1.29	1.68
4	1.69	1.15	1.71	0.8
5	2.21	0.44	2.12	1.77
6	-	-	2.43	0.74
7	3.19	2.83	2.98	1.49
8	3.69	0.65	3.65	0.29
9	4.53	0.64	4.43	0.72
10	4.87	1.09	4.90	0.46
11	6.60	0.39	6.53	0.76
12	8.09	0.22	7.99	0.39
13	10.8	0.55	10.45	9.09

Table 4. Dynamic parameters identified for San Bernardino Interchange.

Mode	Yucaipa		Chino Hills	
	ω (Hz)	ξ (%)	ω (Hz)	ξ (%)
1	0.88	1.18	0.92	3.24
2	0.90	7.32	1.04	10.5
3	1.03	1.49	-	-
4	1.23	0.39	1.33	7.17
5	2.81	3.28	2.71	2.39
6	3.11	6.73	3.01	4.62
7	4.64	3.53	4.66	0.92
8	-	-	4.97	2.25
9	-	-	5.20	4.26
10	6.68	1.76	6.47	1.33
11	-	-	7.22	1.26
12	8.93	0.58	9.17	0.83

The Meloland Road Overpass (MRO) is a reinforced concrete box girder bridge. It consists of two 104 feet spans, constructed monolithically with the abutments and a central circular pier of 5 feet of diameter and 21 feet of height. The pier and the abutments are supported on timber piles. The MRO was constructed in 1971; in 1979 the bridge was instrumented with 26 strong motion accelerometers along the superstructure, base of the pier, embankments and free field. In 1991 the instrumentation was upgraded to 32 sensors (Fig. 4).

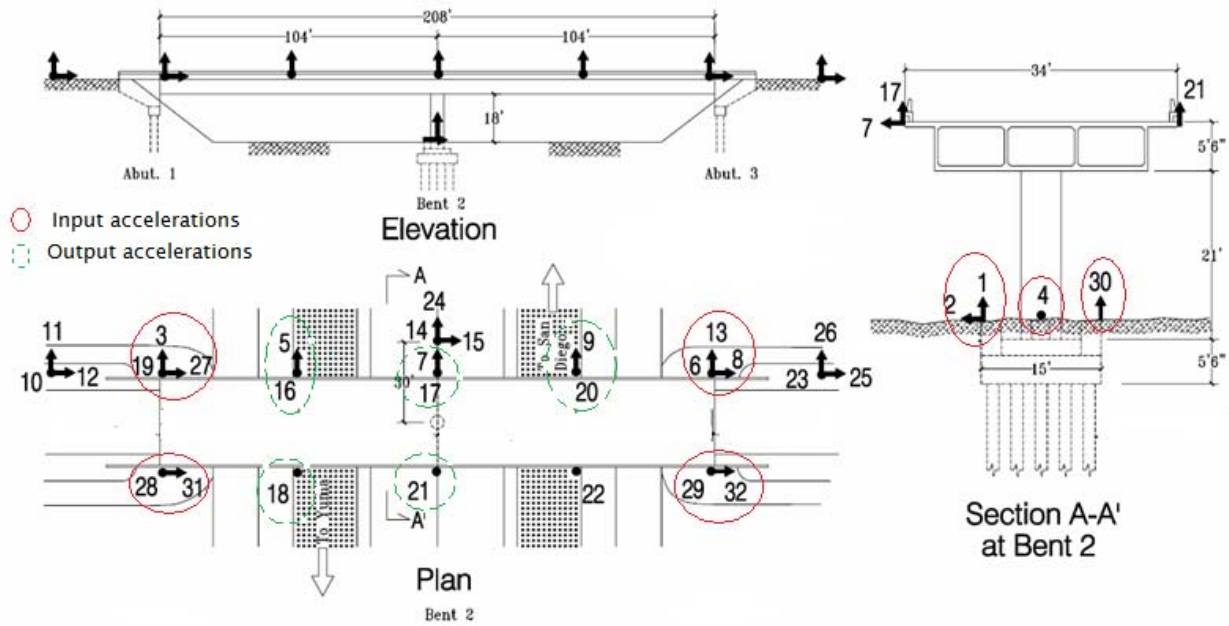


Fig. 4. Elevation and plan views of MRO along with sensor locations

For the system identification of this bridge using ERA/OKID, 14 input acceleration records and 8 output acceleration records were used. The sensors used for the inputs are located at the abutments and at the base of the pier in the three orthogonal directions, while the output sensors are located along the deck of the bridge in the transverse and vertical directions, as shown in Fig. 4. The identification was performed for five ground motions listed in Table 5; all of them were of small magnitude so that a linear behavior was expected.

Table5. Earthquakes used in system identification of MRO

Earthquake	Horizontal Apk (g)		Distance (Km)
	Ground	Structure	Epicenter
Cerro Prieto Feb 8 2008	0.020	0.058	41.9
Cerro Prieto Event 1 Feb 11 2008	0.012	0.035	45
Cerro Prieto Event 2 Feb 11 2008	0.014	0.042	37
Calexico Nov 20 2008	0.017	0.027	50.4
Calexico Dec 27 2008	0.006	0.02	24.5

The identified frequencies and damping ratios are presented in Table 6: for the first three ground motions, six frequencies were identified while, for the remaining two, it was possible to identify only five. The values of the identified frequencies and damping ratios are quite consistent among the five sets: of particular interest is the damping ratio relative to the second frequency that shows consistently high values ranging from 17.40% to 22.79%.

Looking at the time histories of the structural acceleration, extremely good agreement was found between the response predicted by the identified models and the actual recorded response, as can be inferred from the RMS errors for all the channels and ground motions (Table 7). Fig. 5 shows the actual and predicted responses of the bridge at channels 5 and 18 for Cerro Prieto Feb 8 2008.

Table 6. Dynamic parameters identified for MRO

Mode	Cerro Prieto Feb 8 2008		Cerro Prieto Event 1 Feb 11 2008		Cerro Prieto Event 2 Feb 11 2008		Calexico Nov 20 2008		Calexico Dec 27 2008	
	ω (Hz)	ξ (%)	ω (Hz)	ξ (%)	ω (Hz)	ξ (%)	ω (Hz)	ξ (%)	ω (Hz)	ξ (%)
1	3.37	1.12	3.42	1.41	3.43	1.32	3.38	1.49	3.38	1.67
2	4.45	21.4	4.31	21.27	4.47	18.70	3.98	22.79	3.97	17.40
3	4.86	3.6	4.92	2.31	4.90	2.43	4.82	2.79	4.81	3.45
4	7.14	7.4	7.32	5.67	7.29	6.33	7.21	5.18	7.23	6.93
5	10.20	5.8	10.23	4.6	10.15	5.65	9.68	5.49	9.78	6.76
6	14.69	6.15	14.69	9.04	14.79	5.59	-	-	-	-

Table 7. RMS errors of measured data and predicted data by identified models of MRO

Sensor number	RMS error				
	Cerro Prieto Feb 8 2008	Cerro Prieto Event 1 Feb 11 2008	Cerro Prieto Event 2 Feb 11 2008	Calexico Nov 20 2008	Calexico Dec 27 2008
5	0.0328	0.0505	0.0565	0.0793	0.0583
7	0.0258	0.0378	0.0446	0.0628	0.0480
9	0.0330	0.0515	0.0559	0.0849	0.0586
16	0.0804	0.0990	0.0954	0.0939	0.1311
17	0.0718	0.0734	0.0936	0.1137	0.0920
18	0.0832	0.1081	0.1158	0.1044	0.1210
20	0.0806	0.0991	0.0940	0.0861	0.1274
21	0.0736	0.0809	0.1107	0.1267	0.0937

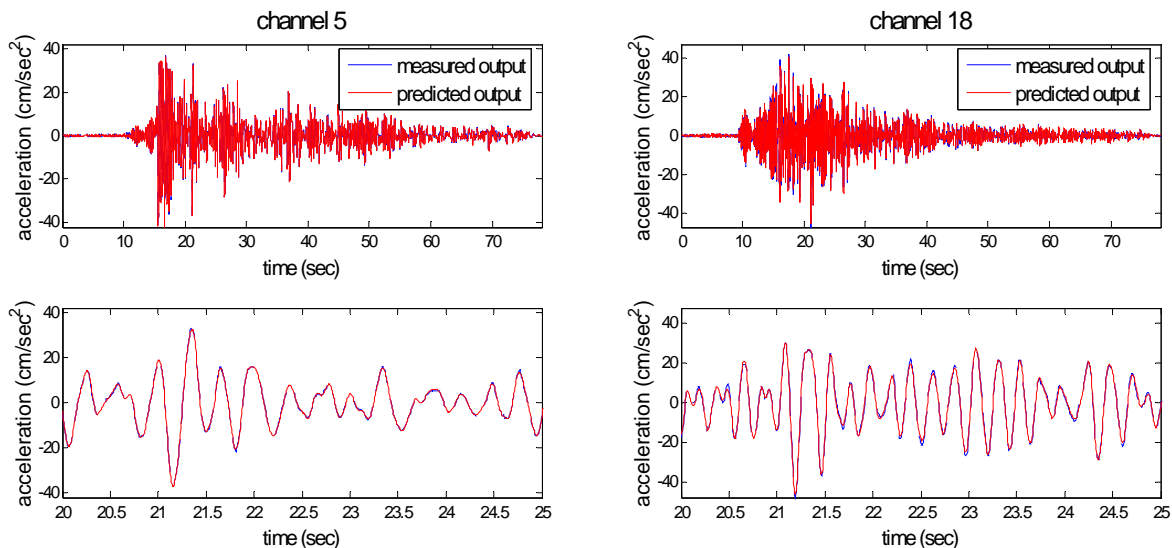


Fig. 5. Recorded and predicted acceleration data for channels 5 and 18 during Cerro Prieto Feb 8 2008 earthquake.

Each identified linear model should be able to reasonably predict the structural response for the other ground motions studied here, since they are of a small intensity and no large

damaging event occurred between these smaller events. The model identified for the input/output data from Calexico Dec 27 2008 was used to predict the structural response obtained with the input data from Cerro Prieto Feb 8 2008. Good agreement was found between the predicted and simulated data; plots for channels five and eight are shown in Fig. 6. The errors found are within acceptable limits.

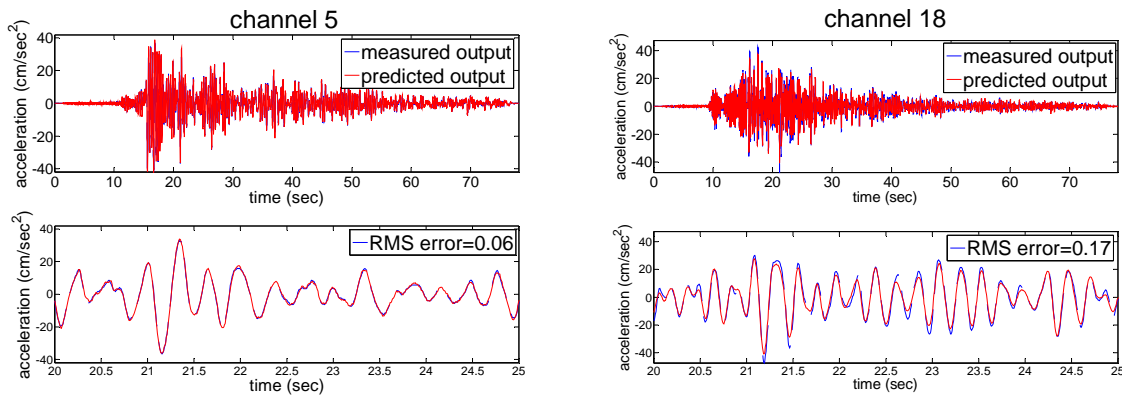


Fig. 6. Recorded and predicted acceleration data for channels 5 and 18 using data from Cerro Prieto Feb 8 2008 earthquake and linear model predicted with Calexico dec 27 2008.

Model updating

An initial finite element model of MRO was developed using SAP2000. The box girder and abutments were modeled with 3776 shells elements and the central pier and bent cap with 24 frame elements. The concrete was assumed to have a unit weight of 0.145 kip/ft³, a Poisson's ratio of 0.2 and a compressive strength of 3250 psi. As input, the displacement time histories from Cerro Prieto Feb 8, 2008, obtained also from the CSMIP website, were applied at the abutments and bottom of central pier.

To be able to accurately identify a reliable model of this bridge structure, the genetic algorithm was used to update the initial SAP2000 model. The objective was to match the frequencies found with ERA/OKID, as well as the measured acceleration time histories along the deck of the bridge with the frequencies and time histories from the FEM model. The fitness function was defined as the sum of the normalized errors of each identified (from ERA/OKID) and simulated (from SAP) frequency plus the sum of the normalized errors between the recorded acceleration time histories and those simulated by SAP.

At each generation of the GA, linear FEM analyses were performed in order to evaluate the fitness function for the new sets of parameters (one per each chromosome). Because of the small magnitude of the earthquake used, a linear analysis was considered appropriate for the model updating, keeping the computational costs low.

The parameters of the model selected to be updated were the elastic modulus of the concrete and the damping ratio parameters. The damping model used here was the Rayleigh damping, which assumes that the damping matrix is proportional to the mass and to the stiffness matrices through two coefficients. The choice of these 3 parameters to be updated was dictated by the fact that there are a lot of uncertainties about their magnitude and that they strongly influence the overall dynamic behavior. A range of possible values was selected for each

parameter. The elastic modulus of the concrete could vary between 460000 ksf and 560000 ksf, the mass coefficient between 0 and 2, and the stiffness coefficient between 0 and 0.01.

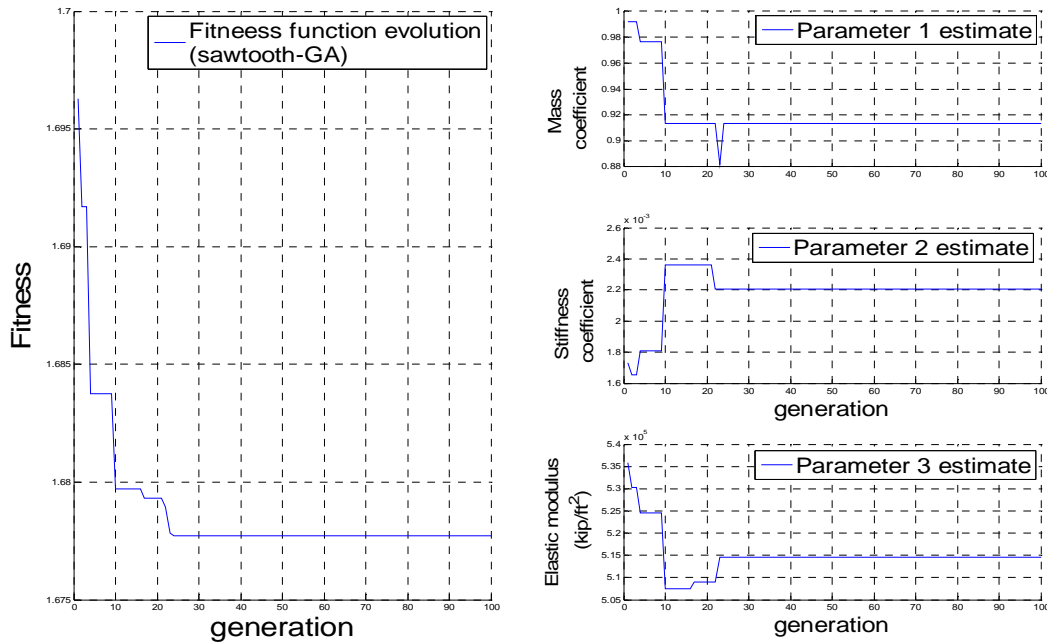


Fig. 7. Fitness function evolution and parameter evolution using genetic algorithm

Evolution of the fitness function and of the three parameters is presented in Fig.7. It was found that the optimized model will have an elastic modulus of 514,645.67 kip/ft² and the mass and stiffness coefficients will be 0.9134 and 0.0022 respectively.

In the Seismic Design Criteria [22] Caltrans suggests the elastic modulus can be approximated by

$$E_c = 57000\sqrt{1.3 * f'_c} \quad (\text{in psi}) \quad (14)$$

which, for an assumed $f'_c = 3250$ psi, corresponds to a magnitude 533,520 ksf. This value is relatively close to the optimal value found in the updating process, e.g. a difference of only 3.5% between them.

To test the accuracy of the updated FEM in reproducing the dynamic behavior of the real bridge, Fig. 8 compares the measured response from the Cerro Prieto Feb 8 2008 earthquake and the simulated one obtained by the updated FEM. Plots for channels 5 and 17 comparing acceleration time history, power spectral density of the acceleration and displacement time history are displayed. From plots, we can see that a good level of agreement was reached with the updating process.

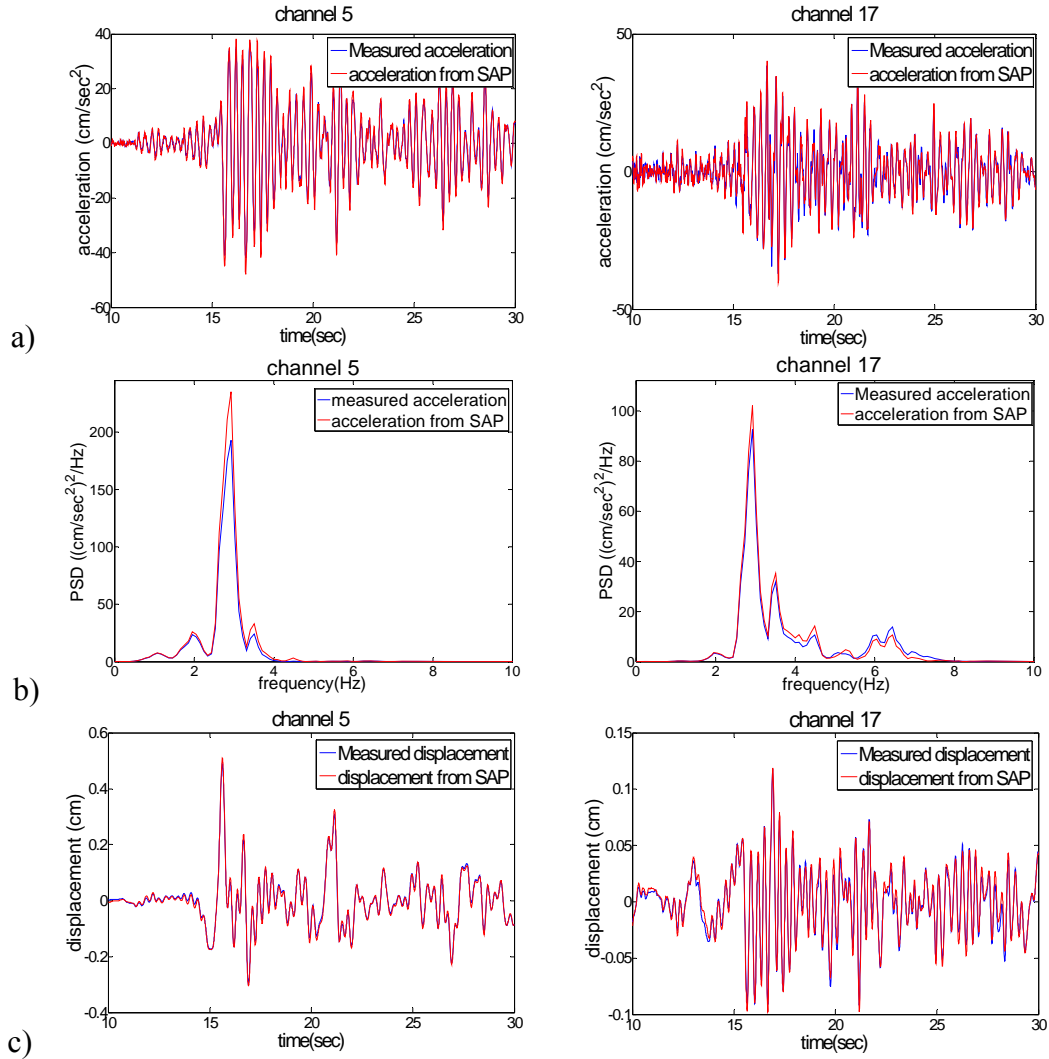


Fig. 8. Comparison of measured response and simulated response by updated SAP model for channels 5 and 7. a) acceleration time history, b) Power spectral density of acceleration, c) displacement time history

Table 8. Frequencies found with OKID and frequencies from FEM after calibration of the model

Mode	Mode description	Frequencies (Hz)	
		Identified with OKID	Calculated with FEM
1	Vertical anti-symmetric mode.	3.37 – 3.43	3.59
2	Transverse mode.	3.98 – 4.47	4.48
3	Vertical symmetric mode.	4.82 – 4.92	5.2
4	First torsional mode.	7.08 – 7.32	7.28
6	Second torsional mode of the whole length of the bridge.	9.68 – 10.2	10.4
10	Third torsional mode of the whole length of the bridge.	14.69 – 14.79	14.2

Table 9. RMS errors of measured data and data simulated by the FEM

Sensor number	Acceleration RMS error	Displacement RMS error
5	0.1576	0.0725
7	0.1416	0.0657
9	0.1633	0.0627
17	0.2252	0.1581
21	0.2345	0.1432
16	0.5218	0.3836
18	0.5584	0.4375
20	0.6462	0.4815

Table 8 shows the frequencies identified with OKID and the ones calculated with the updated FEM and Table 9 presents the RMS error between the measured data and the simulated ones by SAP for displacement and acceleration. From Table 8, it appears that the frequencies of the updated FEM model are within the range of values identified by ERA/OKID, with the exception of the one for mode 3 (slightly higher in FEM model) and the one of mode 10 (slightly lower). In looking at the RMS errors, (Table 9) it can be seen that the updating process was able to simulate the behavior of the first five channels, but it was not able to simulate channels 16, 18 and 20. This larger error on these few channels might be caused by the use of Rayleigh damping in the SAP model. If we compare Rayleigh damping with the values of damping identified by ERA/OKID (Fig. 9.), which is able to accurately predict those channels, we noticed that Rayleigh damping cannot model the damping of the structure for all the modes.

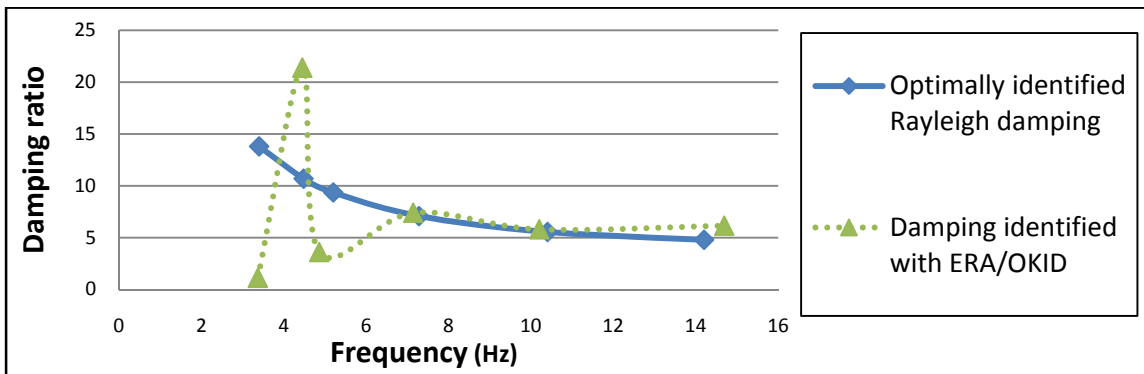


Fig. 9. Comparison damping ratios found using Rayleigh damping and identified by ERA/OKID

Since the acceleration time histories from channels 16, 18 and 20 were not simulated correctly, their data will not be used for the damage assessment.

Nonlinear analysis of the bridge using the updated finite element model

In order to perform a nonlinear analysis, fiber hinges were defined in the model at locations of potential damage as the column-deck and column-foundation connections as well as in the bent cap on each side of the column (Fig. 10). To define the fiber hinges the section of the columns and bent cap had to be divided into a discrete number of fibers. To select the number of fibers for the section, there has to be a balance between accuracy and computational cost: in this study, the column section and bent cap section were divided into four hundred fibers. Cross-sections and fiber distribution of the column and bent cap are shown in Fig. 11.

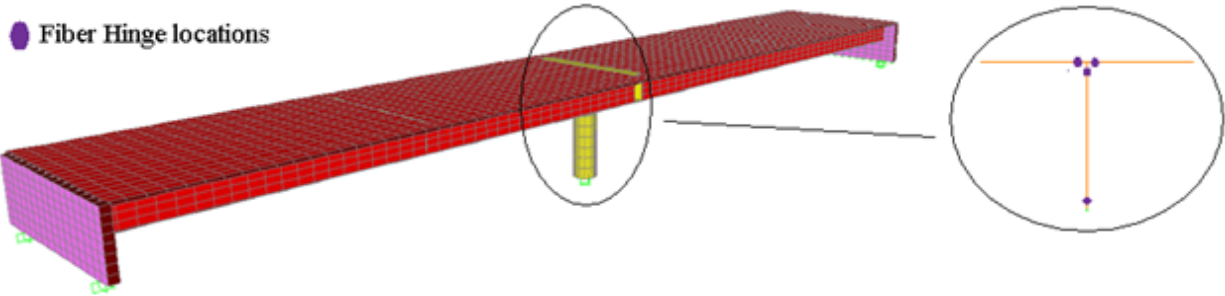


Fig. 10.FEM and fiber hinge locations

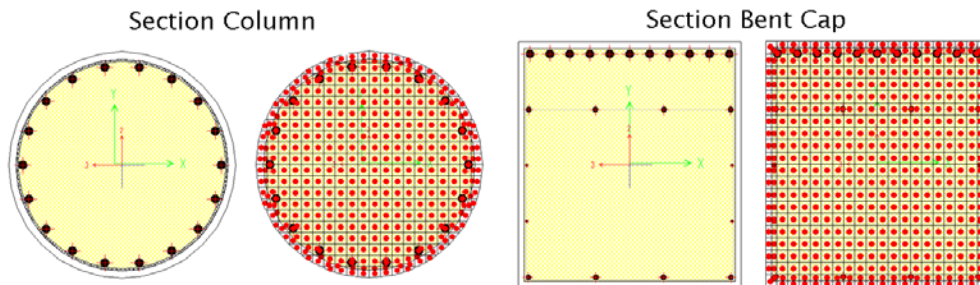


Fig. 11.Section of column and bent cap, and distribution of fibers

The fiber hinge defines its hysteretic behavior through the non-linear material models of the individual fibers [23], [24]; each fiber has a location, a tributary area and a stress-strain curve. For the concrete fibers, the Takeda model [25] was chosen; this model is suitable for concrete and other brittle materials. For the steel fibers, the multi-linear kinematic plastic model [26] was used; such a model is based on the kinematic hardening behavior, commonly observed in metals. Schematic plots of the models are shown in Fig. 12.

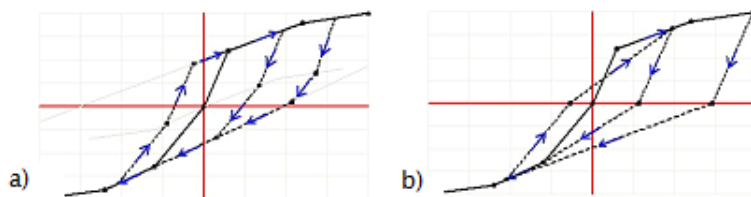


Fig. 12. Hysteretic models. a)Multi-linear kinematic, b)Takeda.

Having decided on the hysteretic behavior of the elements in the FEM, the ground motion time histories from one of the recorded earthquakes available from CSMIP was amplified by different factors and used as input on the FEM model so to induce various levels of nonlinearity on the bridge. These sets of data could simulate ground motions from a damaging earthquake. In Fig. 13 Moment-Rotation diagrams of the hinges at top and bottom of the column are presented for three amplification factors. In case a) the data from Cerro Prieto Feb 8 earthquake has not been amplified, and it is clear that the bridge behaves linearly. In the other two cases shown in Fig. 13, the displacement time histories from Cerro Prieto have been amplified by factors of fifty and one hundred. This amplified displacement time histories correspond to peak ground acceleration of 1.0 g and 2.0 g. For an amplification of fifty, the hinge at the bottom of the column presents nonlinear behavior, while the hinge at the top of the column is only starting to go into the inelastic range. For an amplification of one hundred, both the hinges at top and

bottom of the column clearly show a nonlinear behavior and will both be areas of potential damage. The hinges at the bent cap behave linearly for the first two cases, and start developing some non-linearity in the case where the data is amplified by one hundred.

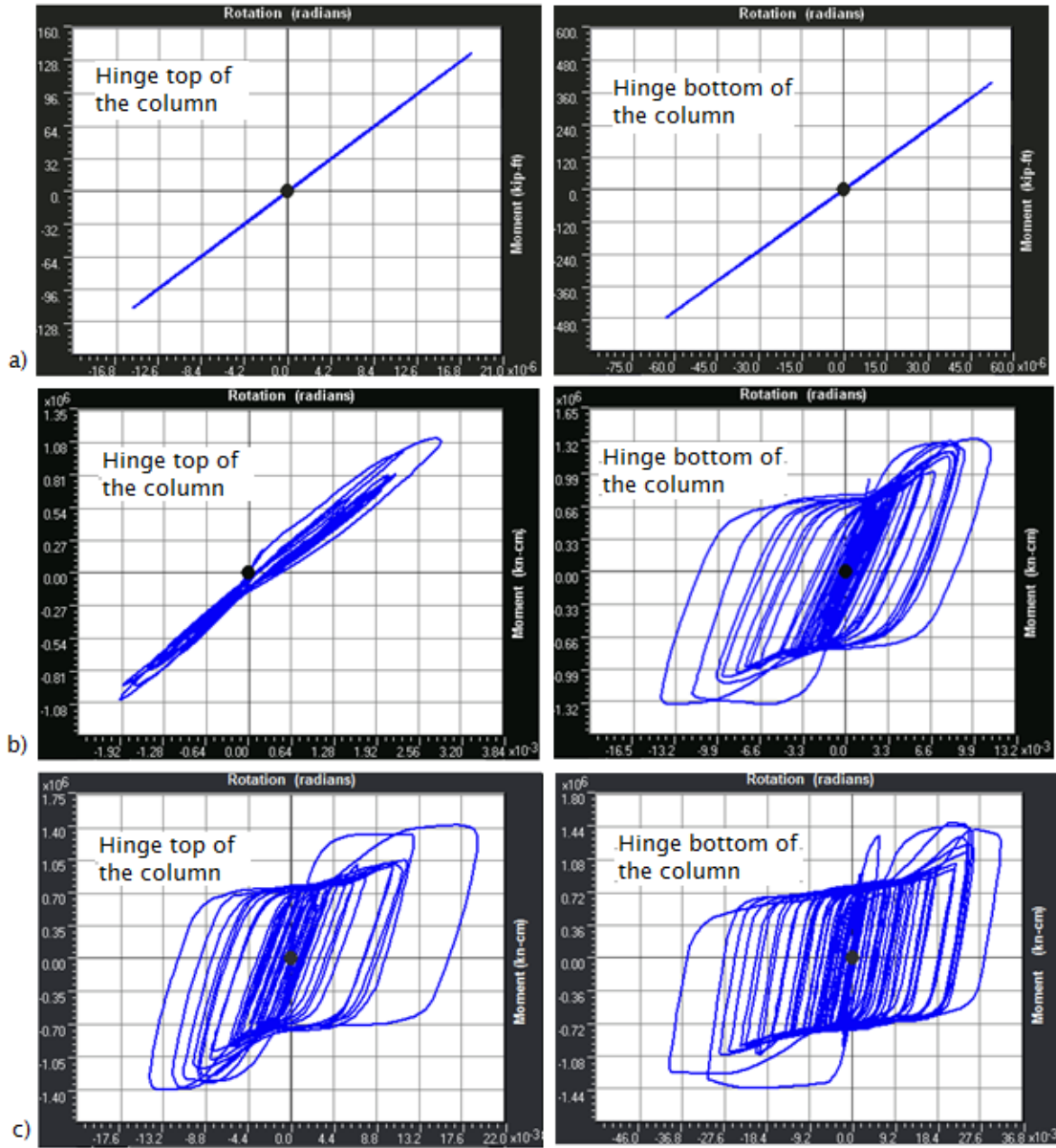


Fig. 13. Moment-Rotation diagrams of hinges at top and bottom of the column for Cerro Prieto Feb 8 Earthquake. a) Without amplification, b) Amplified by 50, c) Amplified by 100.

Table 10. RMS errors of data predicted by ERA/OKID (linear model identified with real data) and data simulated by the FEM

Channel	Acceleration RMS error		
	Original	Amplified by 50	Amplified by 100
5	0.1467	0.3139	0.4198
7	0.1343	0.3514	0.4763
9	0.1510	0.3175	0.4217
17	0.2284	0.3944	0.4600
21	0.2363	0.4042	0.4700

The linear model previously identified with ERA/OKID from the measured accelerations was used to predict the structural response for the different magnitudes of the earthquake. RMS errors of the predicted structural response and the simulated by the FEM are presented in Table 10. It can be seen that the errors increase as the nonlinearity in the structure or level of damage increases.

To show the bases of the damage detection technique used here and assure that the difference in the errors are due to damage in the bridge, a new linear model was determined with ERA/OKID using the data simulated with the FEM model for the case of no amplification of the ground motion. This model was then used to predict the bridge response for the different magnitudes of the earthquake. In Table 11, RMS errors of the data predicted with the linear model obtained with ERA/OKID and the data simulated by the FEM are tabulated. The table shows that, for the original earthquake, the RMS error is quite similar to the one obtained by looking at the real recorded data, an indication that ERA/OKID performs equally well with simulated as well as recorded data. In addition, it shows that the updated FEM model of the bridge provides an accurate representation of the linear behavior of the bridge. The same behavior observed using the linear model identified with ERA/OKID from the measured accelerations occurs here. The errors between the predicted response from the linear model identified with simulated data and the response from the nonlinear model increase as the nonlinearity in the bridge increase.

Table 11. RMS errors of data predicted by ERA/OKID (linear model identified with data simulated by FEM) and data simulated by the FEM

Channel	Acceleration RMS error		
	Original	Amplified by 50	Amplified by 100
5	0.0429	0.2267	0.3474
7	0.0121	0.2755	0.4136
9	0.0409	0.2255	0.3449
17	0.0982	0.2808	0.3391
21	0.1035	0.2945	0.3593

Looking at the time histories of the bridge's deck acceleration, the predicted response is almost identical to the actual response as long as the response remains linear as shown in Fig. 14a, but, as soon as the input is amplified and the response changes from linear to nonlinear, the linear model is no longer capable of predicting the structural response as shown in Fig.14b.

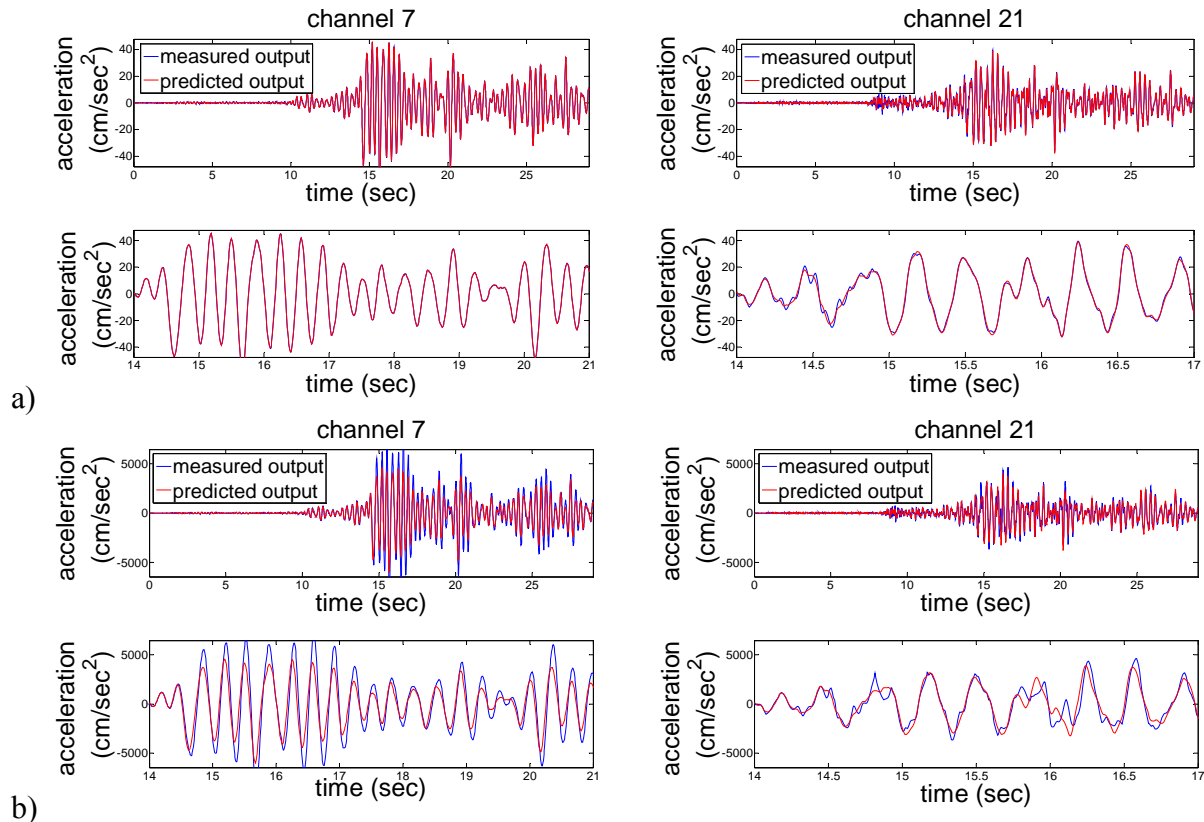


Fig. 14. Comparison of predicted response and simulated response by updated SAP model for channels 5 and 7. a) Acceleration time history, b) Power spectral density of acceleration

Conclusions

This paper presents a vibration-based damage detection technique. The difference between the actual measurement of the structural response and the predicted one by a linear state space model is used to detect damage. The basis of this technique is that a linear model developed using the ERA/OKID system identification technique will correctly predict a linear structural response but, if inelastic behavior (e.g. induced by damage) has occurred, the predicted response will deviate from the actual response.

Initially the ERA/OKID algorithm was applied using time histories of ground shaking and structural response of previous earthquakes. This algorithm, in addition to the high-fidelity linear first-order model later used to detect the presence on damage, provided dynamic characteristics of the structure (e.g. natural frequencies and damping ratios) that were used to update a FEM model of the bridge.

Although most modal updating processes only try to match modal parameters as frequencies and modal assurance criteria, here a more challenging updating process was performed trying to match the measured acceleration time histories at sensor locations, in addition to matching the frequencies of the structure. The numerical results from the updated model showed good agreement with the measured structural response as well as with the modal parameters identified. The model updating process used here shows potential for such a procedure to provide validated structural models of important structures.

The finite element model, updated following a GA, was used to simulate structural response for different levels of input excitation. Consequently, this resulted in increasing levels of structural damage. It was observed that the identified linear model could accurately predict the data if nonlinear behavior is not present, but, as the inelastic behavior grows, the error between the predicted and simulated data also grows.

The procedure used here to identify damage, can be implemented to give an almost immediate damage assessment after a seismic event. If a high-fidelity linear state-space model has been previously identified, when a new ground motion occurs, the data could be processed in near-real time and an estimate of the state of the bridge can be given. This is a rapid tool that can put up a green or red flag in a matter of few minutes after an earthquake.

Acknowledgements

The authors would like to gratefully acknowledge the support and guidance of Dr. Moh Huang and CSMIP which supported this study under contract CSMIP 1007-908. The authors would also like to acknowledge Eleni Chatzi for her guidance with the GA's, Luciana Balsamo for her work on the Rio Dell Overpass and Ah-Lum Hong for her advice on the application of the OKID-based algorithms.

References

- [1] Doebling SW, Farrar CR, Prime MB. A summary review of vibration-based damage detection and system identification methods. *Shock and vibration digest*. 1998; 30(2):91-105.
- [2] Mohamed AS. A data driven approach for earthquake damage detection. Master's thesis, The Graduate School of Natural and Applied Sciences, Atlim University. 2005.
- [3] Smyth AW, Pei JS, Masri SF. System Identification of the Vincent Thomas Suspension Bridge using Earthquake Records. *International Journal of earthquake and Structural Dynamics*. 2003; 32:339-367.
- [4] Lus H, Betti R, Longman RW. Identification of Linear Structural Systems using Earthquake-Induced Vibration Data, *Earthquake Engn. Struct. Dyn*. 1999; 28:918-929.
- [5] Arice Y, Mosalam KM. System identification of instrumented bridges. *Earthquake Engng Struct. Dyn*. 2003; 32:999-1020.
- [6] Juang JN, Pappa RS. An Eigensystem Realization Algorithm for modal parameter identification and model reduction. *J Guid control Dyn*. 1995; 8:620-627.
- [7] Juang JN, Phan M, Horta LG, Longman RW. Identification of observer/Kalman filter Markov parameters: theory and experiments. *J Guid Control Dyn*. 1993; 16:320-329.
- [8] Juang JN. *Applied system identification*. Prentice Hall, 1994.
- [9] Mottershead JE, Friswell MI. Model updating in structural dynamics: a survey. *J Sound Vib*. 1993; 165:347-375

- [10] Brownjohn JMW, Moyo P, Omenzetter P, Lu Y. Assessment of highway bridge upgrading by dynamic testing and finite element model updating. *J Bridge Eng.* 2003;8:162-172.
- [11] Zarate BA, Caicedo JM. Finite element model updating: Multiple alternatives. *Engineering Structures.* 2008; 30: 3724-3730.
- [12] Darrell Whitley. *A Genetic Algorithm Tutorial*, volume 4. 1994.
- [13] Brad L. Miller, Brad L. Miller, and David E. Goldberg. Genetic algorithms, tournament selection, and the effects of noise. *Complex Systems.* 1995; 9:193-212.
- [14] John H. Holland. *Adaptation in natural and artificial systems.* MIT Press, Cambridge, MA, USA. 1992.
- [15] Dudy Lim, Yew-Soon Ong, Yaochu Jin, and B. Sendhoff. Trusted evolutionary algorithm. *Evolutionary Computation. CEC 2006. IEEE Congress.* 2006; 149-156.
- [16] Chang-Yong Lee and Xin Yao. Evolutionary programming using mutations based on the levy probability distribution. *Evolutionary Computation, IEEE Transactions on.* 2004; 8(1):1-13.
- [17] Jinn-Tsong Tsai, Tung-Kuan Liu, and Jyh-Horng Chou. Hybrid taguchigenetic algorithm for global numerical optimization. *Evolutionary Computation, IEEE Transactions on.* 2004; 8(4):365-377.
- [18] Y. W. Leung and Y. Wang. An orthogonal genetic algorithm with quantization for numerical optimization. *Evolutionary Computation, IEEE Transactions on.* 2001;5:41-53.
- [19] David E. Goldberg. Sizing populations for serial and parallel genetic algorithms. 1989;70-79.
- [20] Micro-genetic algorithms for stationary and non-stationary function optimization, 1989.
- [21] C.P. Koumoussis, V.K.; Katsaras. A saw-tooth genetic algorithm combining the effects of variable population size and reinitialization to enhance performance. *Evolutionary Computation, IEEE Transactions on.* 2006;10(1):19-28.
- [22] Caltrans Seismic Design Criteria, Version 1.4, June 2006.
- [23] Filippou FC, Taucher FF. Fiber beam-column for non-linear analysis of RC frames: Part I. Formulation. *Earthquake eng. struct. dyn.* 1996; 25:711-725.
- [24] Filippou FC, Taucher FF. Fiber beam-column for non-linear analysis of RC frames: Part I. Applications. *Earthquake eng. struct. dyn.* 1996; 25:727-742.
- [25] Takeda T, Sozen MA, Nielsen NN. Reinforced Concrete Response to Simulated Earthquakes, *J. Struct. Engrg. Div., ASCE.* 1970; 96(12):2257-2273.
- [26] CSI Analysis Reference Manual for SAP2000, ETABS, and SAFE. April 2009.